Configurational entropy of hard spheres

2007 J. Phys.: Condens. Matter 19 256207

(http://iopscience.iop.org/0953-8984/19/25/256207)

IOP PUBLISHING JOURNAL OF PHYSICS: CONDENSED MATTER

J. Phys.: Condens. Matter **19** (2007) 256207 (9pp) doi:10.1088/0953-8984/19/25/256207

Configurational entropy of hard spheres

Luca Angelani[1] **and Giuseppe Foffi**[2]

[1] Research center SMC INFM-CNR, c/o Università di Roma 'La Sapienza', Piazzale Aldo Moro 2, I-00185, Roma, Italy
[2] Institut Romand de Recherche Numérique en Physique des Matériaux IRRMA, and Institute of Theoretical Physics (ITP), Ecole Polytechnique Fédérale de Lausanne (EPFL), CH-1015 Lausanne, Switzerland

Received 13 April 2007, in final form 16 May 2007
Published 5 June 2007
Online at stacks.iop.org/JPhysCM/19/256207

Abstract

We numerically calculate the configurational entropy $S_{\rm conf}$ of a binary mixture of hard spheres, by using a perturbed Hamiltonian method trapping the system inside a given state, which requires fewer assumptions than the previous methods (Speedy 1998 *Mol. Phys.* **95** 169). We find that $S_{\rm conf}$ is a decreasing function of the packing fraction φ and extrapolates to zero at the Kauzmann packing fraction $\varphi_{\rm K} \simeq 0.62$, suggesting the possibility of an ideal glass transition for the hard-sphere system. Finally, the Adam–Gibbs relation is found to hold.

(Some figures in this article are in colour only in the electronic version)

1. Introduction

The idea that the glass transition is driven by a decreasing of the number of accessible states upon lowering the temperature (or raising the density) is quite old [1–3]. In this picture, if crystallization is avoided, an ideal glass transition is expected to happen at the point where the configurational entropy $S_{\rm conf}$ (the logarithm of the number of states) vanishes. When the liquid enters into the supercooled region, the dynamics becomes slower and slower and the particles get trapped for an increasingly longer time inside the 'cages' made by their neighbours: the dynamics of the system can be successfully described as a 'fast' motion of the representative point in the $3N$ configuration space inside metastable states, and a 'slow' motion corresponding to jumps among states. On entering further into the supercooled region, the number of accessible metastable states decreases and the extrapolation to zero of $S_{\rm conf}$ defines the ideal glass transition. In experiments (or numerical simulations) the region close to the ideal glass transition is unreachable, due to the 'apparent' arrest of the system at the so-called glass-transition temperature (or density) when relaxation times become longer than experimental timescale. The above scenario has been shown to be valid for many interacting systems, based on a smooth pair-potential (such as Lennard-Jones liquids), for which the potential energy

landscape (PEL) approach [4–13] and the replica method [14, 15] have allowed one to give numerical estimations of $S_{\rm conf}$ and of the ideal glass transition.

The overall picture is still not well established for hard spheres (HSs), for which the existence of a glass transition is still an open question [16–20]. A particularly important role seems to be played by the dimensionality of the system. In particular, in $d = 2$ dimensions there are numerical [20, 21] and theoretical [22, 23] evidences of the absence of a thermodynamic glass transition, while the opposite seems to be true for $d = 3$ [18, 24]. Moreover, the step-wise form of the interparticle potential does not allow a PEL analysis, and different approaches have to be taken into consideration in order to calculate the configurational entropy $S_{\rm conf}$. In the past, attempts to estimate $S_{\rm conf}$ have been performed based on different evaluations of the entropy in each single state [18, 25, 26]. Recently the replica method has been extended to the HS case for one-component systems [23, 24].

In this paper we follow an approach, based on the Frenkel–Ladd method [27] and recently introduced in the study of Lennard-Jones systems [28] and attractive colloids [29, 30], to numerically estimate $S_{\rm conf}$ for binary hard spheres. As in previous studies, the calculation is reduced to that of the vibrational entropy $S_{\rm vib}$, using the fact that the total entropy S can be decomposed into the sum of a configurational contribution $S_{\rm conf}$ and a vibrational one $S_{\rm vib}$:

$$S = S_{\rm conf} + S_{\rm vib}. \tag{1}$$

This expression is consistent with the idea that, at high enough density, there are two well-separated timescales: a fast one, related to the motion inside a local state (the rattling in the cage), and a slow one associated to the exploration of different states.

The total entropy S is obtained by thermodynamic integration, starting from the ideal gas state. The quantity $S_{\rm vib}$ is calculated using a perturbed Hamiltonian, adding to the original Hamiltonian an harmonic potential around a given reference configuration. Calculating the mean square displacement from the reference configuration and making an integration over the strength of the perturbation, it is possible to estimate the vibrational entropy [29]. The difference $S - S_{\rm vib}$ provides an estimate of the configurational entropy $S_{\rm conf}$ as a function of packing fraction φ (or density ρ).

The main findings of the present work are the following.

(i) $S_{\rm conf}$ is a decreasing function of the packing fraction φ, and a suitable extrapolation to zero provides an estimate of the ideal phase transition point (Kauzmann packing fraction) $\varphi_{\rm K} \simeq 0.62$.
(ii) The diffusivity D and configurational entropy $S_{\rm conf}$ are related through the Adam–Gibbs relation, in agreement with previous claims [18].

2. The model

The system studied is a binary 50–50 mixture of hard spheres, A and B, with diameter ratio $\sigma_{\rm B}/\sigma_{\rm A} = 1.2$. The collision diameters are $\sigma_{\rm AA} = \sigma_{\rm A}$, $\sigma_{\rm BB} = \sigma_{\rm B}$ and $\sigma_{\rm AB} = (\sigma_{\rm A} + \sigma_{\rm B})/2$. The particles ($N = 256$) are enclosed in a cubic box with periodic boundary conditions. We use the following units: $\sigma_{\rm B}$ for length and $m_{\rm A} = m_{\rm B} = 1$ for mass. Moreover we choose $k_{\rm B} = 1$ and $\hbar = 1$. The density is measured by the packing fraction φ that is related to the number density $\rho = N/V$ by $\varphi = \rho\pi(\sigma_{\rm A}^3 + \sigma_{\rm B}^3)/12$. We analysed systems in the range $\varphi = 0.425$–0.580. Hard-sphere systems depend only trivially on temperature, which sets an overall scale for the dynamics; consequently we perform all our simulations at $T = 1$. We performed standard event-driven molecular dynamics [31] and we stored several equilibrated configurations at different density.

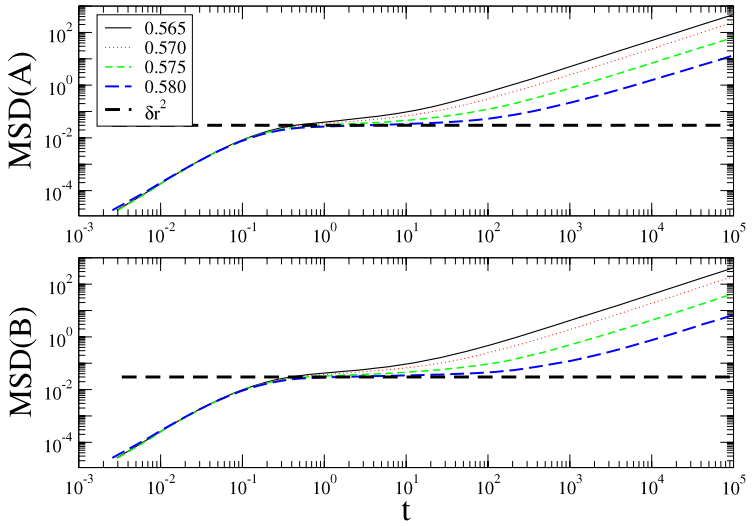

Figure 1. Mean square displacements (MSDs) of species A (top) and B (bottom). Both MSDs has been normalized by the value of the diameter squared. The dashed lines represent the cage size squared, δr^2.

3. Diffusivity

The diffusion coefficients D of the two species have been extracted from the long-time limit of the mean square displacements (MSDs) $\langle r^2(t)\rangle = N^{-1}\langle[\mathbf{r}(t) - \mathbf{r}(0)]^2\rangle$ ($\mathbf{r}$ is the $3N$-vector of the coordinates):

$$\lim_{t\to\infty} \frac{\langle r^2(t)\rangle}{t} \simeq 6D. \tag{2}$$

To improve the statistical significance of the data, an average over ten independent runs was performed. In figure 1 the mean squared displacements for the slowest cases, i.e. $\phi > 0.56$, are presented for both species. It is clear that on increasing the density the MSDs develop the typical two-step relaxation pattern. The first part of the MSD is purely ballistic, while, at a later stage, it reaches the diffusive regime, described by equation (2). Between these two regimes a plateau starts to develop. This is a clear indication of a caging effect. Each particle starts to feel the crowding of its neighbours and it is trapped in a cage for longer and longer time on increasing the density. The height of the plateau is the typical 'cage diameter squared', δr^2. For both species we find $\delta r^2 = 3 \times 10^{-2}\sigma_\alpha^2$ for $\alpha =$ A or B, represented by a dashed line in figure 1. This is clear evidence that the two species have the same caging effect. We shall return to the value of δr^2 later.

In figure 2 the diffusivities D of A and B particles are plotted as a function of the packing fraction φ. Dashed lines in the figure are power-law fits $D = C(\varphi_c - \varphi)^\gamma$ of the high-packing-fraction data ($\varphi \geqslant 0.53$), as predicted by mode-coupling theory. The fitted parameters are $\varphi_c = 0.583$, $\gamma = 2.27$, $C = 9.50$ for A particles and $\varphi_c = 0.583$, $\gamma = 2.47$, $C = 11.66$ for B particles. We note that both diffusivities give rise to the same mode-coupling packing fraction φ_c, in agreement with the prediction of the theory [32] and with previous simulations of the same model [33].

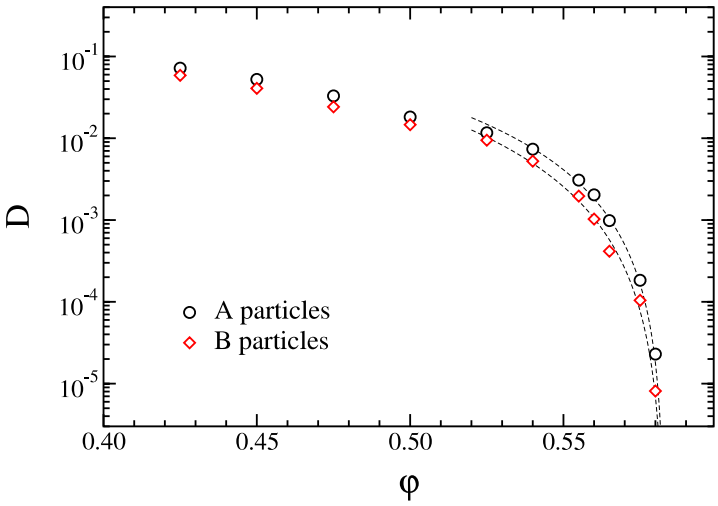

Figure 2. Diffusivity for A and B particles as a function of packing fraction φ. The lines are power-law fits for $\varphi \geqslant 0.53$, $C\ (\varphi_c - \varphi)^\gamma$, with $\varphi_c = 0.583$, $\gamma = 2.27$, $C = 9.50$ for A particles and $\varphi_c = 0.583$, $\gamma = 2.47$, $C = 11.66$ for B particles.

4. Configurational entropy

We now turn to the calculation of configurational entropy. The method we follow to estimate $S_{\rm conf}$ requires the computation of the total entropy S and vibrational entropy $S_{\rm vib}$. The total entropy S is calculated via a thermodynamic integration from an ideal gas and can be expressed as

$$S(\rho) = S_{\rm id}(\rho) + S_{\rm ex}(\rho), \tag{3}$$

where $S_{\rm id}$ is the entropy of the ideal gas and $S_{\rm ex}$ is the excess entropy with respect to the ideal gas. For a binary mixture, the ideal gas entropy is

$$\frac{S_{\rm id}(\rho)}{N} = \frac{5}{2} - \ln\rho - 3\ln\lambda + \ln 2, \tag{4}$$

where $\lambda = (2\pi\beta\hbar^2/m)^{\frac{1}{2}}$ is the de Broglie wavelength ($\hbar$ is Planck's constant and it has been set to unitary value), and the term $\ln 2$ takes into account the mixing contribution. The term $S_{\rm ex}$ can be expressed in the following form:

$$S_{\rm ex}(\rho) = -\frac{N}{T}\int_0^\rho \frac{{\rm d}\rho}{\rho^2} P_{\rm ex}, \tag{5}$$

with $P_{\rm ex}$ the excess pressure. We extracted $P_{\rm ex}$ from the zero-density limit up to the densities of interest, performing numerical simulations and fitting the results of the pressure with a high-order polynomial in ρ. In figure 3 we show the numerically calculated excess entropy $S_{\rm ex}$ (symbols) together with the analytic estimate provided by the Carnahan–Starling (CS) equation of state, extended to hard-sphere mixtures [34, 35][3]. We note that at high densities the CS equation of state overestimates the entropy by about 7%. This discrepancy, however, is not sufficiently significant to affect the resulting $S_{\rm conf}$ values, in particular close to the glass transition.

[3] The analytical CS expression for $S_{\rm ex}$ is given by equation 9 in [35] omitting the last term $\ln Z$, as in our case the excess entropy is defined with respect to the ideal gas at the same density instead of at the same pressure as in [35].

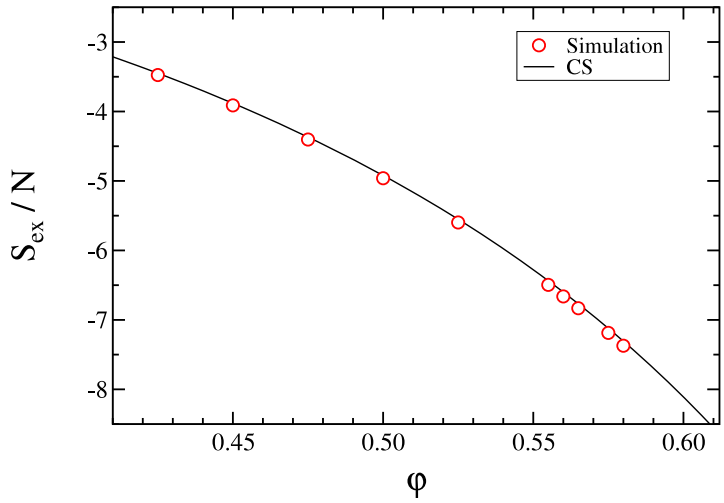

Figure 3. Excess entropy S_{ex} for the mixture of hard spheres as obtained from our simulations (symbols) compared with the analytical Carnahan–Starling expression (line) [35] (see footnote 3).

The method we use for the calculation of S_{vib} is based on the investigation of a perturbed system

$$\beta H' = \beta H + \alpha N(\mathbf{r} - \mathbf{r}_0)^2, \tag{6}$$

where H is the unperturbed hard-sphere Hamiltonian, α is the strength of the perturbation, $\mathbf{r}_0$ specifies the particle coordinates of a reference configuration and $(\mathbf{r} - \mathbf{r}_0)^2 \equiv N^{-1} \sum_{i=1}^{N} (\vec{r}_i - \vec{r}_{0,i})^2$. The reference configuration $\mathbf{r}_0$ is chosen from equilibrium configurations at the considered density (randomly extracted from the stored configurations obtained during molecular dynamics simulations). With this choice one is sure that the estimated vibrational entropy (see the formula below) pertains to the correct state at the studied density. The vibrational entropy can be obtained from the formula (see [29] for details)

$$\frac{S_{vib}}{N} = \int_{\alpha_0}^{\alpha_\infty} d\alpha' \, \langle (\mathbf{r} - \mathbf{r}_0)^2 \rangle_{\alpha'} - \frac{3}{2} \ln\left(\frac{\alpha_\infty \lambda^2}{\pi}\right) + \frac{3}{2}, \tag{7}$$

where $\alpha_{0,\infty}$ are the lower/upper limit of integration, and $\langle \cdots \rangle_{\alpha'}$ is the canonical average for a given α'. The choice of α_0 deserves a few comments. If the system were confined to move inside a given local free-energy minimum, for a correct estimation of S_{vib} one would take the lower limit $\alpha_0 = 0$ in the integral in equation (7). As the system, at a sufficiently low value of α, begins to sample different states (the harmonic force due to the perturbation is no longer able to constrain the system inside one state), α_0 has to be chosen in such a way that the system has not yet left the state: the underlying idea is that equation (7) gives a correct estimation of S_{vib} until the system remains trapped in the state. An appropriate choice in our case seems to be $\alpha_0^{(1)} = 2^{2.5}$ for all the densities, as, close to this point, one observes a crossover for all the investigated densities (more pronounced for low-density data). In figure 4, the quantity $\langle (\mathbf{r} - \mathbf{r}_0)^2 \rangle_\alpha$ is reported as a function of α. An arrow indicates the chosen value $\alpha_0 = \alpha_0^{(1)}$, below which one observes the crossover associated to the exploration of different states.

It is worth noting that different choices of α_0 are in principle possible, giving rise to different estimations of the vibrational entropy term. However, even though a kind of arbitrariness is present in the method, one can argue that a reasonable choice should be for

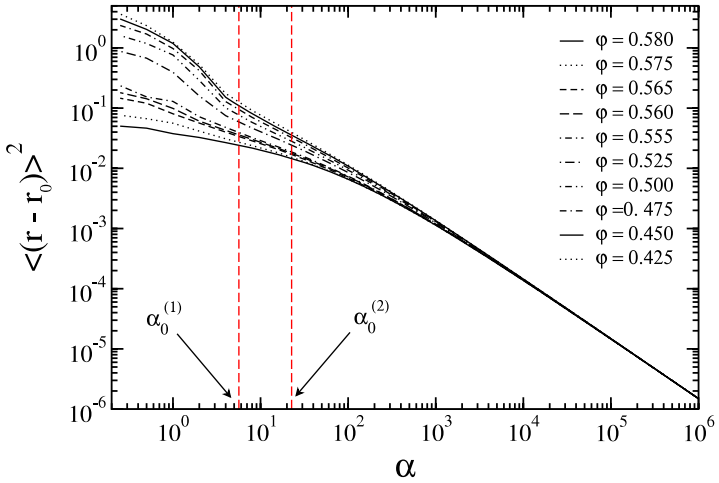

Figure 4. The quantity $\langle(\mathbf{r}-\mathbf{r}_0)^2\rangle_\alpha$ plotted versus α in logarithmic scale for different packing fractions φ. Vertical lines are the values $\alpha_0^{(1)} = 2^{2.5}$ and $\alpha_0^{(2)} = 2^{4.5}$ used as the α_0-value in the integral in equation (7) for the calculation of $S_{\rm vib}$.

values above $\alpha_0^{(1)}$ (close to the crossover corresponding to the exploration of different states) and below an upper value $\alpha_0^{(2)}$ at which one is sure that the system is still confined in a single state. The latter value can be estimated by requiring that the MSD $\langle(\mathbf{r}-\mathbf{r}_0)^2\rangle$ is always close to/below the cage diameter squared $\delta r^2 \simeq 3\times10^{-2}\sigma_\alpha^2$ (with α = A or B) (this has been estimated from the *plateau* of the mean square displacement; see figure 1).

The chosen value in our case is $\alpha_0^{(2)} = 2^{4.5}$ (indicated by an arrow in figure 4). We then repeated the same calculation of $S_{\rm vib}$ using equation (7) with the lower bound in the integral $\alpha_0 = \alpha_0^{(2)}$. In this way we obtain a lower and upper bound for the quantity of interest $S_{\rm vib}$, by using respectively $\alpha_0^{(1)}$ or $\alpha_0^{(2)}$ in the expression for $S_{\rm vib}$ in equation (7).

Figure 5 shows $S_{\rm conf}$ as a function of φ. The configurational entropy $S_{\rm conf}$ is calculated using equation (1), where the two entropies S and $S_{\rm vib}$ are obtained from equations (3) and (7) respectively. Due to the fact that the correct integral for the estimation of $S_{\rm vib}$ should be done from $\alpha_0 = 0$, but with the system always inside a given state, we have added to the expression in equation (7) the term $\alpha_0\langle(\mathbf{r}-\mathbf{r}_0)^2\rangle_{\alpha_0}$, corresponding to assume a constant value of $\langle(\mathbf{r}-\mathbf{r}_0)^2\rangle$ below α_0 and using a zero value for the lower limit of the integral in equation (7). Figure 5 shows the two estimates of $S_{\rm conf}$, corresponding to the two different values of α_0: $\alpha_0^{(1)} = 2^{2.5}$ (open symbols) and $\alpha_0^{(2)} = 2^{4.5}$ (full symbols). One observes that the discrepancy between the two estimations decreases by increasing the packing fraction, suggesting that, at high density, the method used to calculate $S_{\rm conf}$ is less affected by the choice of the free parameters entering in its evaluation. This is probably due to the fact that on increasing the density the system tends to be more trapped in a local free-energy minimum. Indeed, it is only at high density that the method is expected to work better, due to the better definition of two timescales corresponding to local-fast and global-slow dynamics (see figure 1). At low density, instead, the two are less separated and this corresponds to a difficulty in the extrapolation for $\alpha_0 \to 0$ of the quantity reported in figure 4. The low-density data show a clearer crossover on lowering α, and then a worse definition of state in this limit. As we are interested in the high-packing-fraction extrapolation, this fact does not affect our prediction of the Kauzmann density value.

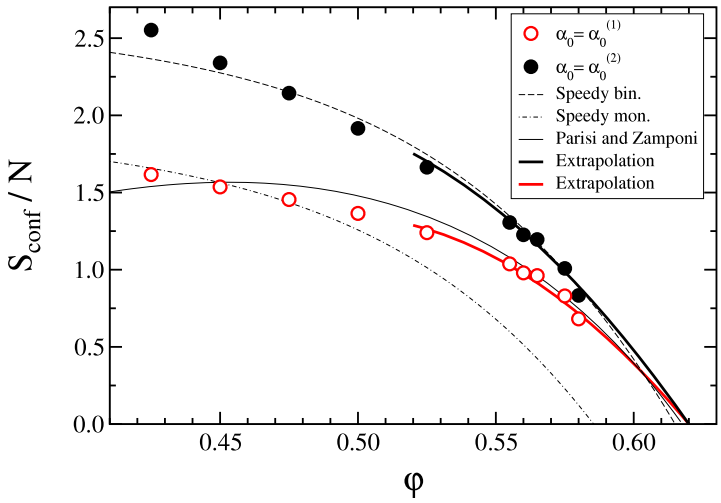

Figure 5. Configurational entropy $S_{\rm conf}$ as function of packing fraction φ. Open symbols are data using $\alpha_0^{(1)} = 2^{2.5}$, full symbols using $\alpha_0^{(2)} = 2^{4.5}$ (see text). Dashed and dot–dashed lines are from Speedy [18] for binary and monatomic hard spheres respectively. The thin full line is the analytical computation of Parisi and Zamponi for monatomic hard spheres [24]. Thick lines are polynomial extrapolations of our data in the high-packing-fraction region, giving rise to the same Kauzmann packing fraction estimation for which $S_{\rm conf}(\varphi_{\rm K}) = 0$: $\varphi_{\rm K} \simeq 0.62$.

Also reported in the figure are the curves obtained by Speedy [18] using a different method (assuming a particular form of the vibrational entropy, a Gaussian distribution of states and involving some free parameters) for the estimation of $S_{\rm conf}$, for monatomic (dot–dashed line) and binary (dashed line) hard spheres (with the same diameter ratio 1.2 and composition 50:50 as in our case). It is worth noting that our method improves on Speedy's one, as, even though requiring some accuracy in the choice of the α_0 parameter, it has the advantage to be less affected by the presence of many free parameters and particular assumptions. We note that the data of Speedy for the binary case do agree very well with our data with $\alpha_0 = \alpha_0^{(2)}$, suggesting the possibility that the choice of $\alpha_0 = \alpha_0^{(2)}$ is more accurate for the estimation of $S_{\rm vib}$ and so of $S_{\rm conf}$. As a comparison, in figure 5 is also reported an analytic estimation of $S_{\rm conf}$ recently provided by Parisi and Zamponi [24] for monatomic hard spheres. From the φ-dependence of the configurational entropy one can determine the packing fraction at which $S_{\rm conf}$ extrapolates to zero, corresponding to the ideal phase transition point (Kauzmann packing fraction $\varphi_{\rm K}$) $S_{\rm conf}(\varphi_{\rm K}) = 0$. Using a polynomial extrapolation[4] for the two sets of data (corresponding to the different α_0 values) we obtain an estimated Kauzmann packing fraction value $\varphi_{\rm K} \simeq 0.62$ (see figure 5). It is worth noting that, even though the two curves are quite different, the estimated value of $\varphi_{\rm K}$ is the same, again suggesting the robustness of the method in the high-density region and then in the estimation of the Kauzmann packing fraction.

5. Adam–Gibbs relation

In this section we explore the validity of the Adam–Gibbs (AG) relation, linking dynamic quantities, like diffusivity, to $S_{\rm conf}$. In figure 6 we report the diffusivities D for A and B particles

[4] We use a polynomial function of the form $A\ (\varphi_{\rm K} - \varphi) - B(\varphi_{\rm K} - \varphi)^2$ to fit the data with $\varphi > 0.5$. Adding more polynomial orders does not significantly affect the extrapolated Kauzmann packing fraction value.

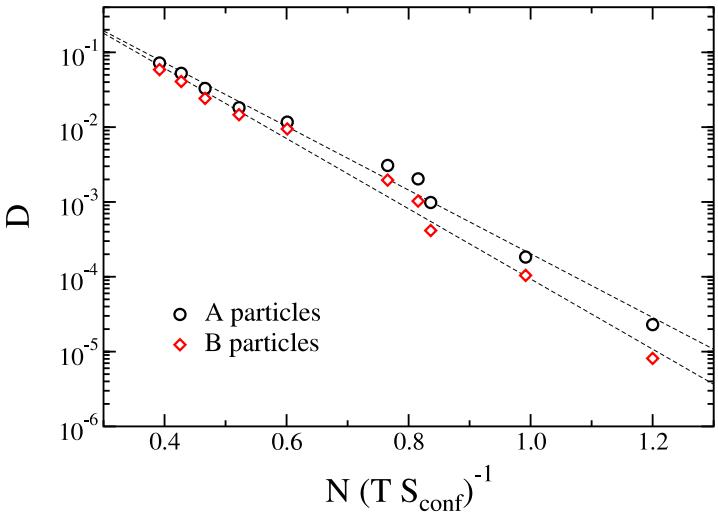

Figure 6. The Adam–Gibbs relation $D = D_\infty \exp[-N\Delta/(TS_{\rm conf})]$ ($T = 1$) for the two species A and B: $D_\infty = 3.66$, $\Delta = 9.8$ for A particles; $D_\infty = 4.59$, $\Delta = 10.8$ for B particles. The data of $S_{\rm conf}$ are obtained with $\alpha_0 = \alpha_0^{(2)}$.

versus the quantity $(TS_{\rm conf})^{-1}$, with $S_{\rm conf}$ obtained for the value $\alpha_0 = \alpha_0^{(2)}$. We find that the Adam–Gibbs relation

$$D = D_\infty e^{-N\Delta/TS_{\rm conf}} \tag{8}$$

is verified (lines in the figure), with $D_\infty = 3.66$, $\Delta = 9.8$ for A particles and $D_\infty = 4.59$, $\Delta = 10.8$ for B particles. A similar behaviour is obtained using $S_{\rm conf}$ calculated with $\alpha_0 = \alpha_0^{(1)}$ (not shown in the figure), with the values $D_\infty = 24.5$, $\Delta = 9.5$ for A particles and $D_\infty = 37.5$, $\Delta = 10.5$ for B particles, suggesting that, in this range of diffusivity values, the AG expression is not able to discriminate between the two different estimations of $S_{\rm conf}$.

6. Conclusions

In conclusion, we have calculated $S_{\rm conf}$ for a binary hard-sphere mixture, by numerically estimating the total entropy S (via thermodynamic integration from an ideal gas) and the vibrational entropy $S_{\rm vib}$ using a numerical procedure based on the Frenkel–Ladd method and recently applied in the analysis of Lennard-Jones systems and attractive colloids: the system is constrained inside a given '*state*' through an harmonic perturbed term in the Hamiltonian. We found, in agreement with analytical and simulation results in the literature, that $S_{\rm conf}$ is a decreasing function of the packing fraction φ, suggesting the possibility of a vanishing of $S_{\rm conf}$ around the Kauzmann point $\varphi_{\rm K} = 0.62$. Moreover, by studying the relationship between $S_{\rm conf}$ and the diffusion constant D, the Adam–Gibbs relation is found to hold reasonably well for the system analysed.

Acknowledgments

We thank G Ruocco, F Sciortino and F Zamponi for useful discussions and suggestions. GF acknowledges the support of the Swiss Science Foundation (Grant No. 200021-105382/1).

References

[1] Kauzmann A W 1948 *Chem. Rev.* **43** 219
[2] Adam G and Gibbs J H 1958 *J. Chem. Phys.* **43** 139
[3] Gibbs J H and Di Marzio E A 1958 *J. Chem. Phys.* **28** 373
[4] Debenedetti P G and Stillinger F H 2001 *Nature* **410** 259
[5] Stillinger F H and Weber T A 1984 *Science* **225** 983
[6] Stillinger F H 1995 *Science* **267** 1935
[7] Sciortino F, Kob W and Tartaglia P 1999 *Phys. Rev. Lett.* **83** 3214
[8] Scala A, Starr F W, La Nave E, Sciortino F and Stanley H E 2000 *Nature* **406** 166
[9] Sastry S, Debenedetti P G and Stillinger F H 1998 *Nature* **393** 554
[10] Büchner S and Heuer A 2000 *Phys. Rev. Lett.* **84** 2168
[11] Sastry S 2001 *Nature* **409** 164
[12] Keyes T 1997 *J. Phys. Chem.* **101** 2921
[13] Sciortino F 2005 *J. Stat. Mech.* P05015
[14] Mézard M and Parisi G 1999 *J. Chem. Phys.* **111** 1076
[15] Coluzzi B, Parisi G and Verrocchio P 2000 *J. Chem. Phys.* **112** 2933
[16] Rintoul M D and Torquato S 1996 *Phys. Rev. Lett.* **77** 4198
Rintoul M D and Torquato S 1996 *J. Chem. Phys.* **105** 9258
[17] Robles M, Lòpez de Haro M, Santos A and Bravo Yuste S 1998 *J. Chem. Phys.* **108** 1290
[18] Speedy R J 1998 *Mol. Phys.* **95** 169
[19] Tarzia M, de Candia A, Fierro A, Nicodemi M and Coniglio A 2004 *Europhys. Lett.* **66** 531
[20] Donev A, Stillinger F H and Torquato S 2006 *Phys. Rev. Lett.* **96** 225502
[21] Santen L and Krauth W 2000 *Nature* **405** 550
[22] Tarzia M 2007 *J. Stat. Mech.* P01010
[23] Zamponi F 2006 *Phil. Mag.* **87** 485
[24] Parisi G and Zamponi F 2005 *J. Chem. Phys.* **123** 133501
[25] Speedy R J 1999 *J. Chem. Phys.* **110** 4559
Speedy R J 2001 *J. Chem. Phys.* **114** 9069
[26] Aste T and Coniglio A 2003 *Physica* A **330** 189
Aste T and Coniglio A 2003 *J. Phys.: Condens. Matter* **15** S803
Aste T and Coniglio A 2004 *Europhys. Lett.* **67** 165
[27] Frenkel D and Smit B 2001 *Understanding Molecular Simulation* 2nd edn (London: Academic)
[28] Coluzzi B, Mézard M, Parisi G and Verrocchio P 1999 *J. Chem. Phys.* **111** 9039
[29] Angelani L, Foffi G, Sciortino F and Tartaglia P 2005 *J. Phys.: Condens. Matter* **17** L113
Foffi G and Angelani L 2007 in preparation
[30] Moreno A J, Buldyrev S V, La Nave E, Saika-Voivod I, Sciortino F, Tartaglia P and Zaccarelli E 2005 *Phys. Rev. Lett.* **95** 157802
[31] Rapaport D C 1997 *The Art of Computer Simulations* 2nd edn (Cambridge: Cambridge University Press)
[32] Voigtmann Th 2003 *Phys. Rev.* E **68** 051401
[33] Foffi G, Götze W, Sciortino F, Tartaglia P and Voigtmann Th 2003 *Phys. Rev. Lett.* **91** 085701
Foffi G, Götze W, Sciortino F, Tartaglia P and Voigtmann Th 2004 *Phys. Rev.* E **69** 011505
[34] Alder B J 1964 *J. Chem. Phys.* **40** 2724
[35] Mansoori G A, Carnahan N F, Starling K E and Leland T W Jr 1971 *J. Chem. Phys.* **54** 1523